

Incommensurate smectic-*A* phase in the general model of frustrated smectic phases

P. Barois

Centre de Recherche Paul Pascal, Domaine Universitaire, 33405 Talence Cedex, France

(Received 20 December 1985)

An incommensurate smectic-*A* phase (SA_i) made of two collinear independent density modulations at two incommensurate wave vectors is found to be stable in the phenomenological model of frustrated smectic phases of Prost in mean-field theory. The N - SA_1 - SA_d - SA_2 - SA_i phase diagram is computed; its representation in appropriate axis (i.e., temperature, incommensurability) is fully compatible with the experimental topology recently reported in a binary mixture of 4-*n*-heptyloxyphenyl-4'-cyanobenzoyloxybenzoate (DB7OCN) and 4-octyloxy-4'-cyanobiphenyl (8OCB).

INTRODUCTION

The rich smectic polymorphism of strongly polar smectogenic compounds¹ is now fairly well understood in the frame of the phenomenological model of frustration of Prost.^{2,3} Uniaxial SA_1 , SA_d , SA_2 (Refs. 4 and 5) as well as biaxial $S\bar{A}$, $S\bar{C}$ (Ref. 3) phases are described in a unified way by two coupled order parameters [usually, but not necessarily referred to as a mass density wave $\rho(\mathbf{r})$ and a polarization wave $Pz(\mathbf{r})$] having a tendency to condense at two incommensurate wave vectors \mathbf{q}_1 and \mathbf{q}_2 , the ratio q_2/q_1 ranging experimentally from 1 to 2. Although incommensurate smectic-*A* phases were among the first to be predicted by the model,² none of them had been discovered until very recently when Ratna, Shashidar, and Raja⁶ reported the first experimental observation of two collinear incommensurate density modulations coexisting in a smectic-*A* phase in a binary mixture of 4-octyloxy-4'-cyanobiphenyl (8OCB) and 4-*n*-heptyloxyphenyl-4'-cyanobenzoyloxybenzoate (DB7OCN).

The aim of this Rapid Communication is to show how the interpretation of this experiment as the first observation of an incommensurate smectic-*A* phase is compatible with the Prost model of frustrated smectic phases in mean-field theory. Unlike in Ref. 2, fourth-order terms are included in

the free energy so that the relative stabilities of the incommensurate smectic *A* and of other uniaxial phases N , SA_1 , SA_d , and SA_2 can be compared.

THE MODEL

As discussed in Ref. 5, uniaxial frustrated smectic phases can be described by two one-dimensionally modulated order parameters:

$$Pz(\mathbf{r}) = \text{Re}[\Psi_1(\mathbf{r})] = \text{Re}[|\Psi_1| \exp(iq_p z)] ,$$

$$\rho(\mathbf{r}) = \text{Re}[\Psi_2(\mathbf{r})] = \text{Re}[|\Psi_2| \exp(iq_p z)] .$$

The z axis is chosen parallel to the nematic director \mathbf{n} , perpendicular to the smectic layers. $\rho(\mathbf{r})$ is the center-of-mass density of the constituent molecules, while $Pz(\mathbf{r})$ describes long-range head-to-tail correlations of polar molecules along the z axis. In the absence of coupling between ρ and Pz , ρ would develop spatial modulations at wave vector $\mathbf{q}_2 = 2\pi/l\mathbf{n}$, where l is of the order of a molecular length, whereas Pz would develop modulations at wave vector $\mathbf{q}_1 = 2\pi/l'\mathbf{n}$, where $l' (> l)$ is a length associated with the pair of antiparallel molecules. In terms of these fields, the Landau free energy of the Prost model reduces in one dimension to

$$\Delta F[\Psi_1, \Psi_2] = \int dz \left[\frac{r_1}{2} |\Psi_1|^2 + \frac{D_1}{2} |(\Delta + q_1^2)\Psi_1|^2 + \frac{u_1}{2} |\Psi_1|^4 + \frac{r_2}{2} |\Psi_2|^2 + \frac{D_2}{2} |(\Delta + q_2^2)\Psi_2|^2 + \frac{u_2}{4} |\Psi_2|^4 + \frac{u_{12}}{2} |\Psi_1|^2 |\Psi_2|^2 - w \text{Re}(\Psi_1^* \Psi_2^*) \right] , \tag{1}$$

where $r_1 = a_1(T - T1)$ and $r_2 = a_2(T - T2)$ and $T1$ and $T2$ are the noninteracting mean-field transition temperatures of the fields $\Psi_1(\mathbf{r})$ and $\Psi_2(\mathbf{r})$, which are expected to depend upon concentration in a binary mixture. The third-order coupling term $-w \text{Re}(\Psi_1^* \Psi_2^*)$ is only relevant if we restrict our attention to slightly overlapping molecules ($1.5 < l'/l < 2$) [a harmonic coupling term $-w' \text{Re}(\Psi_1 \Psi_2^*)$ is required in the other limit $1 < l'/l < 1.5$ (Ref. 2)].

In addition to the three phases discussed in Ref. 5, namely, the nematic (N) with $|\Psi_1| = |\Psi_2| = 0$, the monolayer smectic *A* (SA_1) with $|\Psi_1| = 0$, $|\Psi_2| \neq 0$, and the bilayer smectic *A* (SA_2) with $|\Psi_1| \neq 0$, $|\Psi_2| \neq 0$, and $q_p = q_0$, $q_p = 2q_0$, we now look for the simplest incommensurate

structure (SA_i) defined by $|\Psi_1| \neq 0$, $|\Psi_2| \neq 0$, and $q_p \neq 2q_0$, i.e., only two modes coexisting at incommensurate wave vectors. It follows immediately from the incommensurability of q_p and q_0 that the coupling term $-w \text{Re}(\Psi_1^* \Psi_2^*)$ oscillates along the z axis, and thus averages to zero in the SA_i phase. The minimization with respect to wave vectors is then straightforward and gives $q_p = q_1$ and $q_p = q_2$. After an appropriate rescaling of variables,⁵ we are left with a reduced free energy analogous to the one describing the bicritical-tetracritical problem:⁷

$$f(SA_i) = y_1 x_1^2 + (1 + \delta u_1) x_1^4 + y_2 x_2^2 + (1 + \delta u_2) x_2^4 + 2x_1^2 x_2^2 , \tag{2}$$

with

$$x_1 = \frac{u_{12}}{8w} \left(\frac{D_1}{D_2} \right)^{1/2} |\Psi_1|, \quad y_1 = \frac{r_1}{2} \frac{u_{12}}{w^2}, \quad (1 + \delta u_1) = \frac{16u_1}{u_{12}} \frac{D_2}{D_1},$$

$$x_2 = \frac{u_{12}}{2w} |\Psi_2|, \quad y_2 = \frac{r_2}{32} \frac{u_{12}}{w^2} \frac{D_1}{D_2}, \quad (1 + \delta u_2) = \frac{u_2}{16u_{12}} \frac{D_1}{D_2}.$$

In mean field, the stability of the incommensurate (or intermediate) phase ($x_1=0$ and $x_2=0$) in the third quadrant $y_1 < 0, y_2 < 0$ depends on the coefficients of the fourth-order terms. The case $(1 + \delta u_1)(1 + \delta u_2) > 1$ (i.e., $u_1 u_2 < u_{12}^2$) will only be investigated since the other condition allows no incommensurate phase⁷ to appear in mean-field theory and obviously corresponds to Ref. 5.

The phase ($x_1=0, x_2 \neq 0$) is stable in the $y_1 > 0, y_2 < 0$ region and clearly identifies to SA_1 , whereas a phase ($x_1 \neq 0, x_2=0$) that we call SA_x appears in the $y_2 > 0, y_1 < 0$ region. We know from Ref. 5 that SA_x is always of higher energy than SA_2 because of the third-order coupling term,^{4,5} but close to SA_d (i.e., SA_2 with $x_1 \gg x_2$). The incommensurate phase is stable in the third quadrant in a region limited by two second-order transition lines: $y_1 = y_2 / (1 + \delta u_2)$ SA_1 - SA_i line and $y_1 = (1 + \delta u_1)y_2$ SA_i - SA_x line. The free-energy density of the incommensurate phase is easily minimized to

$$f(SA_i) = \frac{2y_1 y_2 - y_1^2 (1 + \delta u_2) - y_2^2 (1 + \delta u_1)}{4[(1 + \delta u_1)(1 + \delta u_2) - 1]}$$

and the phase diagrams are finally obtained by comparing $f(SA_i)$ to $f(N)=0, f(SA_1) = -y_2^2 / [4(1 + \delta u_2)]$, and the computed value of $f(SA_2)$ in the same rescaled dimensionless units.⁵

PHASE DIAGRAMS

We choose $\delta u_1 = 9, \delta u_2 = 0$. The strength of the incommensurability is measured as in Ref. 5 by the reduced parameter

$$z = (u_{12} D_1 / 2)^{1/2} (q_1^2 - q_2^2 / 4) / w$$

proportional to the difference of natural wave vectors over the coupling constant w . For small incommensurability parameter z (Fig. 1), the origin $y_1 = 0, y_2 = 0$ is deep in the SA_2 phase, there is no bicritical point, and SA_2 is always found to be of lower energy than SA_i . The diagram is qualitatively similar to Fig. 3(b) of Ref. 5. Rotated axes $(y_1, y_2) \rightarrow (t, x)$ are introduced to show the close agreement with the experimental diagram of the DB_nOCN series (Fig. 1 of Ref. 8) as it was already noticed in Refs. 3 and 4.

For higher incommensurability parameter $z > z_c$ given in Ref. 5 [$z_c = 1/(6)^{1/2}$ here] (Fig. 2), the bicritical point B appears and SA_i is found to be stable in a quasitriangular domain which grows when increasing z . The SA_1 - SA_i second-order line is given by Eq. (2) $y_1 = y_2 / (1 + \delta u_2)$, while SA_2 - SA_i and SA_d - SA_i are first order. Of course, SA_x and the SA_x - SA_i line never appear. Even with rotated axis, the topology of the theoretical diagram in the (y_1, y_2) plane at constant z (Fig. 2) is far from the experimental one in the (DB7OCN-8OCB) plane. Moreover, the discontinuity at the SA_d - SA_2 transition unambiguously grows when moving along the line towards the SA_i phase, whereas it decreases in the experiment.⁶ It is in fact clear that the (y_1, y_2) (or rotated t, x) representation at constant incommensurability

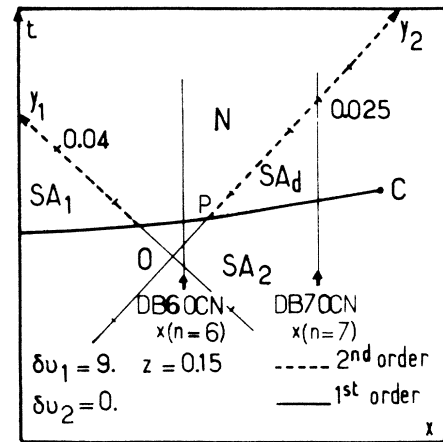


FIG. 1. N - SA_1 - SA_d - SA_2 phase diagram in the case of a small incommensurability parameter z . The incommensurate phase does not appear. Rotated axes (t, x) are introduced to emphasize the close topological similarity with the experimental diagram of the DB_nOCN series (Ref. 8): t corresponds to the temperature and x to the concentration in binary mixtures of successive homologous compounds. Pure products $n=6, n=7$ can be easily located on both sides of the critical end point P , whereas calorimetric and x-ray data of Ref. 8 allow one to estimate that the critical point C is not far from $n=8$. The pure DB7OCN axis ($t, n=7$) is thus defined as $t = 2(5)^{-1/2}(y_2 - 0.025) + (5)^{-1/2}y_1$.

parameter z is not appropriate to describe a DB7OCN-8OCB mixture, since the ratio of the two natural lengths $l'/l = q_2/q_1$ considerably varies from DB7OCN (l'/l close to 2) to 8OCB (l'/l close to 1). It follows from its definition that the incommensurability parameter z must increase significantly from DB7OCN to 8OCB.

We thus suggest that a theoretical phase diagram should be represented in a (t, z) coordinate system to be compared to the experimental one.⁶ Such a diagram is shown in Fig.

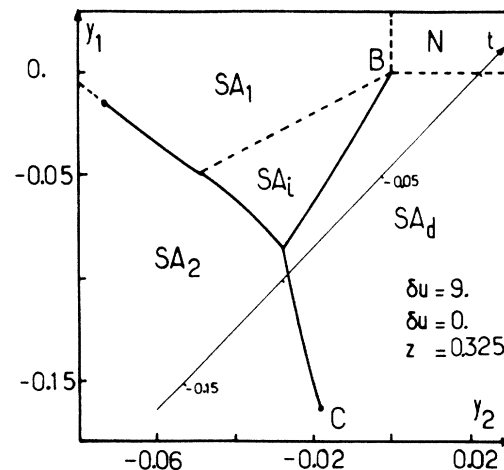


FIG. 2. N - SA_1 - SA_d - SA_2 - SA_i phase diagram in the case of higher incommensurability parameter ($z > z_c$). The rotated $(t, n=7)$ axis of Fig. 1 is mentioned again, but the topology is quite different from that of the experimental diagram of Ref. 6. The nearly triangular SA_i domain grows when increasing z and crosses the above defined $(t, n=7)$ axis for $z > 0.36$.

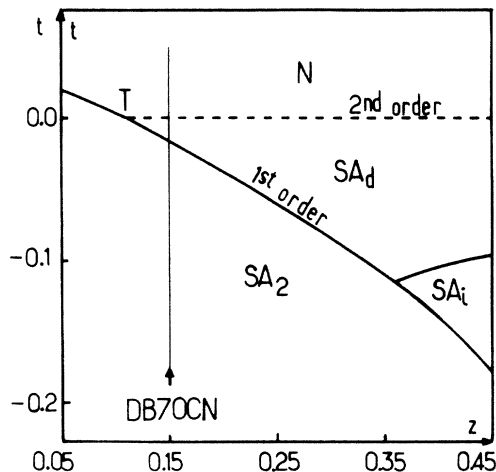


FIG. 3. N - SA_d - SA_2 - SA_i diagram in the (t, z) plane. x has the constant value defined in Fig. 1 for $n=7$ so that pure DB7OCN is characterized by the same set of parameters in Figs. 1 and 3 ($z=0.15$). The z axis is clearly related to the experimental concentration of 8OCB in DB7OCN (Ref. 6).

3, with t defined by the same rotation as in Fig. 1 and $x(n=7)$ and $z(=0.15)$ corresponding to pure DB7OCN (i.e., the DB7OCN axis of Figs. 1 and 3 are common, as required). The topology is now in excellent agreement with the experiment.⁶ Moreover, values of z lower than 0.15 are investigated to show the critical end point T where the three phases N , SA_d , SA_2 meet. This point does enter a $(t, z > 0.15)$ representation at constant $x(n=6)$ (see Fig. 1), and thus should be reached in a DB6OCN-8OCB binary diagram.

CONCLUDING REMARKS

We have shown that the original observation of an incommensurate smectic- A phase is fully compatible with the topology computed from the Prost model of frustrated smectics in a temperature-incommensurability parameter cross section of the phase space. Other experimental features can be interpreted the following way:

(1) The lack of a harmonic coupling term in the free energy (1) makes it possible to describe the DB7OCN-rich part

of the diagram only since it requires $1.5 < l'/l < 2$ as already mentioned. Fortunately, the experimental diagram of Ref. 6 corresponds to this limit [$X(8OCB) < 40\%$].

(2) The choice of the (t, x) coordinate system from the original (y_1, y_2) is not critical to get the topology of Fig. 3 provided that the t axis crosses the SA_2 - SA_d line (as in Figs. 1 and 2). Depending on the exact definition of t (and of the value of other parameters $\delta u_1, \delta u_2$) the discontinuity (i.e., the latent heat) along the first-order SA_2 - SA_d line can either increase or decrease, as experimentally seen,⁶ when moving towards SA_i . Although it is not impossible *a priori*, an exact cancellation of the discontinuity at the triple point SA_d - SA_2 - SA_i is, however, unlikely in the present approach.

(3) The SA_d - SA_i and SA_i - SA_2 lines are necessarily found to be first order because of the single-mode approximation of the incommensurate structure. For finite values of the coupling constant w , a modulated structure consisting of a periodic stack of discommensurations is known to be more stable² and allows the SA_i - SA_d and SA_i - SA_2 transitions to be continuous⁹ as probably observed.⁶ Moreover, the absence of any modulated structure in the x-ray scattering data⁶ suggests that the coupling constant w is weak. Thus, if one forgets about the discontinuity, the evolution of wave vectors reported in Ref. 6 is in agreement with the present model (see formula 2-11 of Ref. 5): $q_0(SA_d)$ increases to q_1 at the SA_d - SA_i transition, $2q_0(SA_2)$ decreases to q_2 at the SA_2 - SA_i transition.

At last, we must mention that the existence of the incommensurate phase close to the bicritical or tetracritical point B ($y_1=y_2=0$) in the (y_1, y_2) plane (Fig. 2) is not correctly predicted by mean-field theory, but depends on the sign of the specific-heat exponents α associated with the second-order N - SA_1 and N - SA_d lines.^{7,10} If α is negative as expected from theory (inverted XY universality class¹¹), B is tetracritical and the incommensurate phase should always be present (i.e., the mean-field topology of Fig. 2 is valid close to B). If α is positive, B is bicritical and the incommensurate phase should not reach it. In both cases, however, the incommensurate SA_i domain of Fig. 3 is far enough from the origin B to believe that mean-field theory has some relevance.

ACKNOWLEDGMENTS

The author would like to thank J. Prost for helpful discussions and critical reading of the manuscript.

¹For a review see, for example, F. Hardouin, A. M. Levelut, M. F. Achard, and G. Sigaud, *J. Chim. Phys.* **80**, 53 (1983).

²J. Prost, in *Proceedings of the Conference on Liquid Crystals of One- and Two-Dimensional Order and Their Applications, Garmisch-Partenkirchen, 1980*, edited by W. Helfrich and G. Heppke, Springer Series in Chemical Physics, Vol. II (Springer-Verlag, Berlin, 1980), p. 125.

³J. Prost and P. Barois, *J. Chim. Phys.* **80**, 65 (1983).

⁴J. Prost, *J. Phys. (Paris)* **40**, 581 (1979).

⁵P. Barois, J. Prost, and T. C. Lubensky, *J. Phys. (Paris)* **46**, 391 (1985).

⁶B. R. Ratna, R. Shashidar, and V. N. Raja, *Phys. Rev. Lett.* **55**, 1476 (1985).

⁷M. E. Fisher and D. R. Nelson, *Phys. Rev. Lett.* **32**, 1350 (1974); A. D. Bruce and A. Aharony, *Phys. Rev. B* **11**, 478 (1975); J. M. Kosterlitz, D. R. Nelson, and M. E. Fisher, *ibid.* **13**, 412 (1976).

⁸F. Hardouin, M. F. Achard, Huu Tinh Nguyen, and G. Sigaud, *J. Phys. (Paris) Lett.* **46**, 123 (1985).

⁹P. G. de Gennes, *Solid State Commun.* **6**, 163 (1968); W. L. McMillan, *Phys. Rev. B* **14**, 1496 (1976).

¹⁰Jiang Wang and T. C. Lubensky, *J. Phys. (Paris)* **45**, 1653 (1984).

¹¹J. Toner, *Phys. Rev. B* **26**, 462 (1982).